Conductivities of a quantum Hall system with a model disorder potential: Influence of electron-phonon interaction on plateau widths

D. Bicout
Laboratory of Chemical Physics, NIDDK, Building 5, Room 136, National Institutes of Health, Bethesda, Maryland 20892

P. Magyar and J. Riess
Centre de Recherches sur les Très Basses Températures, associé à l'Université Joseph Fourier, Centre National de la Recherche Scientifique, Boîte Postale 166, 38042 Grenoble Cedex 9, France

(Received 26 August 1996; revised manuscript received 26 November 1997)

We consider noninteracting electrons in a quasi-two-dimensional strip (extended in the x direction) in the presence of a strong perpendicular magnetic field and a constant electric field in the y direction, and subject to a model disorder potential $V(x,y)$ (''toy model'') which allows us to obtain the exact solutions of the time-dependent Schrödinger equation in very good approximation. Further, the electrons are coupled to a heat bath (accoustic phonons) at temperature T that modifies the coherent Schrödinger time evolution induced by the electric field E_y. After elimination of macroscopically unobservable fluctuations by averaging over suitable short time intervals, the time evolution that is relevant for the macroscopic current density can be described by a Boltzmann-type equation, which is solved numerically. The steady-state solution allows us to calculate σ_{yy} and σ_{xy} as a function of any physical parameter of the system. Here we give results of σ_{yy} and of σ_{xy} for all filling factors and as a function of temperature. Quantized Hall plateaus are obtained at the correct values with high precision. Between two plateaus, the Shubnikov–de Haas peak spreads out and its maximum decreases with increasing temperature in qualitative accordance with typical quantum Hall samples. Further, we obtain the remarkable result that for temperatures below 5 K the plateaus of σ_{xy} become sensibly larger than those of σ_{yy}. Our analysis shows that this effect results from electron-phonon interaction. (Such a phenomenon has been known experimentally for a long time, but it has seemed unexplained so far.) Our method of calculation could, in principle, be extended to more complex disorder potentials. [S0163-1829(98)02612-5]

I. INTRODUCTION

It is generally believed that the integer quantum Hall effect[1] (IQHE) is due to a localization-delocalization process caused by disorder in the presence of a high magnetic field. When the Fermi energy is shifted the two-dimensional electron system changes from insulating behavior (with no dissipation) at quantized Hall conductance plateaus to dissipative, ''metallic'' behavior between the plateaus. In recent years considerable experimental and theoretical effort has been made to achieve a better understanding of this transition between adjacent conductance plateaus.[2–4]

The task for the theory of the IQHE is to give a deductive microscopic explanation of the localization-delocalization phenomenon and the resulting quantization of the Hall conductivity. Further, any satisfactory quantitative theory has to predict the width of the conductivity plateaus as well as the detailed form of the conductivities between them (as a function of temperature and other physical parameters). But such a theory is still missing (Ref. 3, pages 6 and 120). The aim of this paper is to develop such a theory for electrons in a simplified disorder potential (a class of model disorder potentials to be specified in Sec. II).

The major difficulty of the theory of the IQHE lies in the fact that the *true microscopic behavior* of the electrons in the usually rather complex disorder potential is not sufficiently known. (This is illustrated by the statement[5] that ''the microscopic nature of the transport remains rather unclear.'')

In recent years progress in overcoming these deficiencies has been made, which has revealed new aspects[6] in the understanding of the IQHE. These investigations have been carried out along two lines. (1) Some pertinent *general* properties of the *exact* solutions of the Schrödinger equation of a quantum Hall system have been established. This has shown the importance of the time dependence of the wave functions in the presence of a disorder potential and of a macroscopic electric field **E** and that the latter is an important parameter, which has to be included properly in the Schrödinger equation (a restriction to terms linear in **E** is not sufficient for small **E**); for a review, see Ref. 6(i). (2) These general results have been illustrated and confirmed by explicit calculations for a class of model systems[6(a)–6(f)] characterized by simplified disorder potentials, which are chosen such that the solutions of the time-dependent Schrödinger equation and the particle velocities can be calculated explicitly in very good approximation. For these model systems, the microscopic processes behind the occurance of the quantized conductivity plateaus can be understood in detail.

In the present paper we will extend the work of Refs. 6(a)–6(f) such that the Hall and dissipative conductivities can be calculated also *outside the conductivity plateaus*. To this end the interaction with the heat bath (phonons) will be included. We will use the same type of disorder potential $V(x,y)$, as previously,[6(a)–6(f)] since here the Schrödinger time evolution of the states in the presence of a macroscopic electric field can be calculated in very good approximation. The aim of our model calculation is first of all conceptional: to understand the nature of the microscopic processes in a

 © 1998 The American Physical Society

quantum Hall system, in particular, the interplay between the electron-phonon interaction and the Schrödinger time evolution induced by the macroscopic electric field. Further, in the framework of our model system, to show how a microscopic theory can be made without major approximations or unproved assumptions. Finally, we hope to obtain new insight into observable effects, which otherwise (previously) could not have been obtained.

The remainder of this paper is organized as follows. Section II is devoted to the presentation of the model system, followed by a short description of the Schrödinger dynamics of the electrons, where reference is made to earlier work on the subject. In Sec. III, we consider the interaction of phonons with the electrons of Sec. II, and derive the associated electron-phonon transition probabilities. In Secs. IV and V, we set up the Boltzmann equation in a form adapted to our model, with the appropriate field and collision terms taken from the previous two sections. We then show how to calculate the dissipative and Hall currents and the corresponding conductivities, pointing out some peculiarities that differ from the treatment of more conventional situations. Section VI discusses the computer results obtained for the model, and relates the data to available experiments. Finally, in Sec. VII, we conclude by emphasizing the conceptual clarity and particular aspects of the present theory, and outline some possible extensions.

II. DESCRIPTION OF THE ELECTRON SYSTEM

We consider noninteracting electrons (charge $e<0$) on a long strip in the x direction (of width L_y in the y direction) in the presence of a perpendicular strong magnetic field $\mathbf{B}=(0,0,B)$, a macroscopic electric field $\mathbf{E}=(0,E_y,0)$ and a static disorder potential $V(x,y)$. We consider the one-electron Hamiltonian,

$$H=(1/2m)\left\{\left(\frac{\hbar}{i}\frac{\partial}{\partial x}\right)^2+\left[\frac{\hbar}{i}\frac{\partial}{\partial y}-(e/c)[Bx+\phi(t)/L_y]\right]^2\right\}+V(x,y), \tag{1}$$

with periodic boundary conditions in the y direction, where $\phi(t)=-cE_yL_yt$. The Hamiltonian (1) describes a subdomain in the bulk of a macroscopic sample.

In typical quantum Hall systems the potential $V(x,y)$ is thought of as being composed of a smooth part $V^s(x,y)$, which varies slowly over the magnetic length $\lambda_B=|\hbar c/eB|^{1/2}$, and a more rapidly varying part, say, $V^1(x,y)$. In the absence of V^1, the static wave functions in a high magnetic field can be approximately described semiclassically, by wave functions centered on equipotential lines of $V^s(x,y)$. A macroscopic electric field $\mathbf{E}$ causes the guiding centers of the approximate, semiclassical orbitals to move in a direction perpendicular to $\mathbf{E}$ with an additional velocity component $\mathbf{v}_d=(c/B^2)\mathbf{E}\times\mathbf{B}$ [in addition to the local Hall velocity arising from the local electric field $-(1/e)\,\mathrm{grad}\,V^s(x,y)$]. Now one has to distinguish between *two different basic situations, as follows*.

(a) The orbitals are on a tangential surface *parallel* to $\mathbf{v}_d$. In this case they are approximated by *stationary* solutions of the Schrödinger equation in the presence of an infinite potential slope (with periodic boundary conditions parallel to $\mathbf{v}_d$), which have fixed guiding centers localized in a direction perpendicular to $\mathbf{v}_d$. They describe electrons with a total *classical* velocity $\mathbf{v}_d-(c/B^2)(1/e)\,\mathrm{grad}\,V^s(x,y)\times\mathbf{B}$. *The energetic positions (*i.e., *in the z direction) of the guiding centers remain unchanged in the course of time*. Note that the velocity components $-(c/B^2)(1/e)\,\mathrm{grad}\,V^s(x,y)\times\mathbf{B}$ do not contribute to the *macroscopic* current. They average to zero, since for each slope an opposite exists. What remains are the classical velocity components $\mathbf{v}_d$. If a small $V^1(x,y)$ is added, this situation does not change appreciably, since the new solutions become stationary linear combinations of the unperturbed Landau functions on the same slope or on opposite slopes.

(b) The basis orbitals are on tangential surfaces *parallel to the direction of* $\mathbf{E}$: In this case *their energies go up or down with time, depending on the sign of grad* $V^s(x,y)$. Let us now add a small $V^1(x,y)$ and consider two orbitals on opposite slopes. The total time evolution can then become entirely nonclassical in the direction of $\mathbf{v}_d$, leading to velocities that may be much larger than the classical drift velocity $\mathbf{v}_d$ [Refs. 6(a)–6(f)]. This leads to the so-called compensating current, which is a key element in the IQHE.

Further, because of their different energy changes in the presence of $\mathbf{E}$, orbitals on opposite slopes parallel to $\mathbf{E}$ can be populated differently (in the steady state). Therefore, the velocity components parallel to $\mathbf{E}$ are here not necessarily averaged to zero on a macroscopic level.

For an investigation of this crucial case (b), we consider now a simplyfied disorder potential

$$V(x,y)=V(x)+V^1(x,y). \tag{2}$$

Here $V(x)$ is a sequence of slowly varying barriers and wells (obstacles) [Fig. 5; see also Fig. 1 of Refs. 6(b) and 6(f)], and $V^1(x,y)$ is a more rapidly varying part that has to be considered as a perturbation of $V(x)$, with Fourier coefficients [specified in Ref. 6(f), see below]

$$d_k(x)=(1/L_y)\int V^1(x,y)\exp[i2\pi yk/L_y]dy,\quad k \text{ integer}. \tag{3}$$

$V(x)$ simulates long-range fluctuations, which we restrict to the x direction in the present model calculation. This has the advantage that there exist only tangential planes in the direction parallel to $\mathbf{E}=(0,E_y,0)$ and that the solutions in the absence of V^1 are very well approximated by Landau functions [associated with tangential planes at the *straight*, horizontal equipotential lines of $V(x)$], whose guiding centers move perpendicularly to $\mathbf{E}$, with the classical velocity $\mathbf{v}_d=(cE_y/B,0,0)$. Further, if V^1 is added (its detailed form is not important, provided it is sufficiently small, see below) the time dependent solutions can be obtained in a very good approximation as well. The form (2) may be called a ''toy model'' for the more complex disorder potential in usual quantum Hall samples.

The solutions of the time-dependent Schrödinger equation will be expanded as

$$\psi^j(x,y,t)=\sum_p c_p^j(t)\,\psi_p(x,y,t), \tag{4}$$

where

$$\psi_p(x,y,t)=(L_y)^{-1/2}\exp(i2\pi py/L_y)u_p(x,t), \quad p \text{ integer} \tag{5}$$

are the Landau functions centered at

$$x_p(t)=chp/(eBL_y)-\phi(t)/(BL_y)-m^*c^2V'(x_p)/(e^2B^2), \tag{6}$$

and V' denotes $dV(x)/dx$. In this article we generally consider a single Landau band, associated with the lowest Landau level ($n=0$); hence the Landau index n has been droped in Eq. (5).

If $\phi(t)$ varies slowly, that is to say, if the field E_y is sufficiently small, all solutions of the time-dependent Schrödinger equation with Hamiltonian (1) become adiabatic[7] solutions, i.e., eigenfunctions of $H[\phi(t)]$, where the time t is considered to be a parameter.

In the absence of $V^1(x,y)$ the functions $\psi_p(x,y,t)$ are approximate adiabatic solutions [if x_p is not too close to the top of a peak or to the bottom of a valley of $V(x)$]. The corresponding energies are

$$E_p(t)=\hbar\omega_c(n+1/2)+V[x_p(t)]+(m^*/2)[cV'(x_p)/(eB)]^2. \tag{7}$$

These energies $E_p(t)$, $E_{p'}(t)$ increase or decrease, respectively, as a function of t, depending on the sign of $V'[x_p(t)]$. This leads to a spectrum of intersecting energy levels [see Fig. 1 of Ref. 6(f)].

In the presence of $V^1(x,y)$ (the y dependence is important) the adiabatic energy levels $\varepsilon_s(t)$ of $H[\phi(t)]$ *anticross* and are individually periodic as a function of ϕ with period $hc/|e|$ [see, e.g., Fig. 2 of Ref. 6(b)]. The velocity expectation values (in both the y and x directions) of adiabatic states are periodic in time with period $\tau=h/|eE_yL_y|$, and their average over the period τ is zero.[8] Since τ is very small for physically realistic values of E_yL_y, this means that adiabatic states do not contribute to the macroscopic current.

In our model the physical parameters $V'(x)$ and $V^1(x,y)$ are now chosen such that all states *in the central range of the broadened Landau band* can be described by a *weak disorder approximation*.[6(a)–6(c)] This leads to adiabatic states $w(x,y,t)$, which are time-dependent linear combinations of only *two* Landau functions $\psi_p(x,y,t),\psi_{p'}(x,y,t)$, which are situated on opposite slopes of $V(x)$. The resulting adiabatic wave functions oscillate between opposite slopes with time period τ [see, e.g., Fig. 3 of Ref. 6(a)], which corresponds indeed to a vanishing dc current.

For sufficiently high values of E_y *nonadiabatic transitions* become possible between certain adiabatic states [see Fig. 3 of Ref. 6(b)]. In our weak disorder case the probabilities for these nonadiabatic transitions take the explicit form[6(d)–6(f)]

$$P_{pp'}=\exp\{-|4\pi^2|d_{p\text{-}p'}|^2 \times\exp[-2(x_p-x_{p'})^2/(2\lambda_B)^2]B/[V'(x_p)chE_y]|\}. \tag{8}$$

Here $4\pi^2|d_{p\text{-}p'}|^2\exp[-2(x_p-x_{p'})^2/(2\lambda_B)^2$ is just the matrix element $|\langle p|V^1(x,y)|p'\rangle|^2$, where $x_p=x_p(t^*)$, $x_{p'}=x_{p'}(t^*)$ are situated on *opposite* sides of a barrier (well) such that $E_p(t^*)=E_{p'}(t^*)$. $P_{pp'}$ is the probability to go during the time interval $\tau/2$ from a state ψ_p situated at $x_p(t)$ to a state situated at $x_p+(x_{p+1}-x_p)/2$ (i.e., on the *same* slope), and $1-P_{pp'}$ is the probability to go to a state $\psi_{p'}$ which has the same energy, but whose position $x_{p'}$ is on the nearest *opposite* slope. These transition probabilities only depend on the energy of intersection E $[=E_p(t^*)]$ of the levels $E_p(t),E_{p'}(t)$. In Fig. 1 of Ref. 6(f) the energies of intersection are denoted by $E_j, j=0,\pm1,\pm2,\ldots$. Hence we can define $P_j=P(E_j)$.

We use the same parameter values as in Ref. 6(f), except $V'=1.15\times10^3$ eV cm^{-1} and $|d_{p\text{-}p'}|^2=0.6\times10^{-6}$ (eV)^2, which are slightly different. The resulting probabilities P_j remain equal to those in Ref. 6(f). They decrease from $P_j=1$ in the very band center to $P_j=0$ at the *mobility edges* $E_j=\pm E_b$, see Fig. 1 of Ref. 6(f). In the intermediate energy zones, where $0<P_j<1$, the time evolution of a wave function is the result of successive splittings (described by 2×2 matrices) at the ''anticrossing times'' $t=n\tau/2$, n integer, see Fig. 2 of Ref. 6(d) and Fig. 1 of Ref. 6(f). Thus any state with initial condition $\psi(x,y,t=0)=w_s(x,y,0)$ with energy ε_s in the nonadiabatic, i.e., in the *conducting range* $[-E_b,E_b]$ becomes for $t\gg\tau/2$ a *time-dependent* linear combination (4) with much more than two nonzero coefficients $c_p(t)$ associated with energies $E_p(t)\in[-E_b,E_b]$. On the other hand, states with energies outside the conducting range $[-E_b,E_b]$ remain adiabatic (i.e., insulating), and they do not mix with the conducting states.

Our model system thus fulfills the basic requirements of a quantum Hall system,[9] i.e., there exist conducting states in the center and insulating states in the tails of a broadened Landau band.

For further details the reader is referred to Refs. 6(a)–6(f). Note that in Ref. 6(f) (inset of Fig. 1) the distance L across a barrier or well was denoted by L_x, and the origin of t was chosen such that each orbital $w_s(x,y,t=0)$ [with energy $\varepsilon_s(0)$] coincides with an orbital ψ_p [with energy $E_p=\varepsilon_s(0)$] and the notation ε_p was used for this energy E_p.

III. ELECTRON-PHONON SCATTERING

In a heterojunction [or in a metal-oxide-semiconductor field-effect transistor] (MOSFET), the coherent dynamics of the electron system described in Sec. II is influenced by the interactions with the phonons of the surrounding crystal. Below, the phonon modes will be taken to be those of bulk GaAs.[10] We will mainly focus on the temperature range between ~1 K and liquid He temperature, say, where most experiments are done. This allows us to discard piezoacoustic (PA) scattering (which is known to be significant only at very low T)[11] and scattering with LO phonons (which is only expected to play a role for $T>40$ K). Therefore, we will specialize to the case of deformation potential scattering.

Given that the calculations will be restricted to a region around half-integer filling, at the temperatures considered above, the electrons cannot make inter-Landau-level (LL) transitions. Further, we do not pursue the investigation of the dependence on the LL index, so in line with Sec. II and

many theoretical approaches, we assume that only the lowest LL is occupied, and drop the LL index in our expressions.

We multiply the wave functions $\Psi(x,y)$ of Sec. II by the Fang-Howard trial wave function[12] in the z direction,

$$\Psi(z)=\left(\frac{1}{2\lambda_z}\right)^{1/2} z\ \exp\left(\frac{-z}{2\lambda_z}\right). \tag{9}$$

This enables us to include the effect of the finite width of the 2 DEG in our final expressions for the conductivities (although this will not be investigated in detail in the present article).

In general, an electron which initially occupies the state ψ_p interacts with the surrounding heat bath (here acoustic phonons at temperature T), and makes a transition to another state $\psi_{p'}$ that involves the emission or the absorption of a phonon with energy $\hbar\omega_{\mathbf{q}}$ and wave vector $\mathbf{q}$. The first-order probability $\omega^{(e\text{-}p)}_{np,np'}$ per unit time for this transition is given by the Fermi golden rule,[13] which contains the corresponding electron-DA phonon matrix element $M^{\mathbf{q}}_{p,p'}$.[14,15]

There are many possible $\mathbf{q}$ vectors that have the same magnitude and the same y component, which scatter the electron from the initial state $k_y(p)=2\pi p/L_y$ to the same final state $k_y(p')=2\pi p'/L_y$. Their contributions must be added together. This gives an additional multiplicative factor, which is calculated in Appendix A. The resulting—partially summed—transition probabilities can then be written in the form

$$W^{(e\text{-}p)}_{p,p'}=\overline{I}(\tilde{q}_y,\alpha_{p,p'},\lambda_z)F(\tilde{q}_y,\alpha_{p,p'})(n_{\mathbf{q}}+\tfrac{1}{2}\pm\tfrac{1}{2}), \tag{10}$$

where $\overline{I}$, F, $\alpha_{p,p'}$, and $\tilde{q}_y$ are defined in Appendix A and $n_{\mathbf{q}}$ is the equilibrium (Bose-Einstein) distribution of the phonons at temperature T and the upper (lower) sign stands for emission (absorption).

In Ref. 14 electron-phonon interaction in a quantum Hall system with a smooth disorder potential $V(x,y)$ was investigated by replacing the potential by an infinitely extended tangential surface (a single potential slope with average steepness). The semiclassical wave functions associated with the potential lines of $V(x,y)$ were simulated by Landau functions. The resulting electron–acoustic-phonon scattering rate showed a linear temperature behavior for a wide range of temperatures, corresponding to an effective reduction of the Debye temperature, which was traced back to the wave-function shrinkage due to the high magnetic field (resulting in the exponentially decaying factor in our Eq. (A6). Based on a number of more intuitive arguments, this result was then used to describe the temperature behavior of the width of the transition region between quantum Hall plateaus.

In contrast to our paper, Ref. 14 does not discuss the time evolution of the Schrödinger solutions induced by a macroscopic electric field $\mathbf{E}$. Further, no slope changing processes are considered. However, for the calculation of a macroscopic current induced by an electric field $\mathbf{E}$ slope changing processes play an important role as our calculations will show. We are not aware of similar calculations performed elsewhere.

IV. MACROSCOPIC CURRENTS AND THE BOLTZMANN EQUATION

For the description of the macroscopic current it is sufficient to know the microscopic properties at the very closely spaced discrete times $n\tau$. τ is the time interval during which the center of a function $\psi_p(x,y,t)$ moves from $x_p(t)$ to the extremely close adjacent position $x_{p+1}(t)$ (if the centers x_p are numbered consecutively). We then have $x_p(t+\tau)=x_{p+1}(t)$ and $E_p(t+\tau)=E_{p+1}(t)$. Therefore, in the following we use as basis functions the set of time-independent functions $\psi_p(x,y,t=0)\equiv\psi_p$ with their positions x_p and energies E_p [instead of the time-dependent basis functions $\psi_p(x,y,t=n\tau)$]. This is analogous to the method of quasiclassical dynamics for Bloch electrons in an electric field,[16] where the set of time-independent Bloch functions $\psi_{\mathbf{k}}(\mathbf{r})$ is used as basis functions, which are just the corresponding time-dependent adiabatic Schrödinger functions taken at $t=0$.[17]

The total occupation numbers of the basis states ψ_p will be denoted by $f_p(t)$. They result from the (coherent) Schrödinger time evolution induced by E_y and the (irreversible) time evolution caused by the interaction with the phonons. The Schrödinger evolution alone can be calculated (at the discrete times $n\tau$) by multiple applications of complex 2×2 matrices (see Sec. II). However, for the calculation of the *macroscopic* current densities (of a macroscopic sample) the knowledge of the probabilities $P_{pp'}$ and $1-P_{pp'}$, i.e., of the absolute squares of the matrix elements, is sufficient.

One reason is that the conductance fluctuations that might result from the phases of the matrix elements are averaged out when the contributions from different obstacles [hills and valleys of $V(x)$] are summed up. It is like averaging over a number of mesoscopic samples. (The phases of the matrix elements of the 2×2 matrices contain the phases of the $V^1_{pp'}$, which are random[6(c)] and different at different obstacles of a macroscopic sample.) [Note that already for processes within a *single* obstacle the phases are irrelevant in the following important cases: (a) If scattering with phonons occurs only after a time interval much longer than $\tau/2$, the possible phase effects are averaged out because of phase randomization[6(c)] during the Schrödinger evolution itself. (b) If scattering occurs within a time interval τ (two splittings or less), the coherent Schrödinger time evolution in this short interval is not affected by phase effects, since no superposition of contributions from different paths in the energy time plane occurs.[6(c)] This concerns the states near the Fermi level. (c) When the Fermi level is contained in a nonconducting range and the temperature is sufficiently low such that the conducting states below the Fermi level are not scattered by the phonons, the Hall current is entirely due to these conducting states. The Hall conductivity is then quantized, see Sec. 5 of Ref. 6(i), where a general proof is given. This proof is (partly) based on charge density invariance at times $n\tau$. In our weak disorder case, this invariance results already from the absolute values of the 2×2 splitting matrice elements [as one can see from the splitting scheme, e.g., Fig. 1 of Ref. 6(f) and hence is independent of the phases.]

As a consequence, the occupation numbers $f_p(t)$ can be obtained from the following *Boltzmann rate equation:*

$$\partial f_p/\partial t=\sum_{p'}\{-f_p(1-f_{p'})W^{(e\text{-}p)}_{p,p'}+f_{p'}(1-f_p)W^{(e\text{-}p)}_{p',p}\}$$

$$+\sum_{p'}\{-f_pW^{\mathrm{Sch}}_{p,p'}+f_{p'}W^{\mathrm{Sch}}_{p',p}\}. \tag{11}$$

Here $W^{\mathrm{Sch}}_{p,p'}$ is the transition rate from a basis state ψ_p (localized at x_p, with energy E_p) to a state $\psi_{p'}$ (localized at $x_{p'}$, with energy $E_{p'}$) due to the Schrödinger time evolution. For the calculation of the macroscopic current it is sufficient to define $W^{\mathrm{Sch}}_{p,p'}$ as the average transition probability per unit time, averaged over the small time interval τ. In this way the possible temporal fluctuations that arise from the admixture of adiabatic processes (which are periodic within the very short time interval τ and hence are macroscopically irrelevant) are averaged out. The probabilities $W^{\mathrm{Sch}}_{p,p'}$ can be expressed in terms of the Zener transition probabilities $P_{pp'}$, Eq. (8), see Appendix B.

The current in the y direction results from the Schrödinger velocities

$$v^j_y(t)=\partial_t\langle\psi^j|H|\psi^j\rangle/eE_y. \tag{12}$$

In our weak disorder approximation we have [see also Ref. 6(f)]

$$\sum_j\langle\psi^j|H|\psi^j\rangle(n\tau)=\sum_p f_p(n\tau)E_p. \tag{13}$$

From this and Eq. (12), expressing the time derivative of the occupation numbers f_p by the Schrödinger part of Eq. (12), one obtains the macroscopic current density in y direction (at $t=n\tau$, n integer) as

$$j_y(t)=\sum_p f_p(t)\sum_{p'}W^{\mathrm{Sch}}_{p,p'}(E_{p'}-E_p)/(2LL_yE_y). \tag{14}$$

Equation (14) can be written in a different, maybe more familiar way in terms of the velocities v^p_y associated with the basis function ψ_p, see Appendix C.

The macroscopic *Hall current density* j_x results from summing over all single-particle velocities in the x direction, which can be expressed in terms of the transition rates $W^{\mathrm{Sch}}_{p,p'}$ and $W^{(e\text{-}p)}_{p,p'}$ between the positions x_p. One obtains

$$j_x(t)=[e/(2LL_y)]\sum_{\substack{p,p'\\ |x'_p-x_p|<L}}f_p(t)[W^{\mathrm{Sch}}_{p,p'}+W^{(e\text{-}p)}_{p,p'}(1-f_{p'}(t))](x_{p'}-x_p)$$

$$+[e/(2LL_y)]\sum_{\substack{p,p'\\ x_{p'}-x_p>L}}f_p(t)[W^{\mathrm{Sch}}_{p,p'}+W^{(e\text{-}p)}_{p,p'}(1-f_{p'}(t))](x_{p'}-x_p-2L)$$

$$+[e/(2LL_y)]\sum_{\substack{p,p'\\ x_p-x_{p'}>L}}f_p(t)[W^{\mathrm{Sch}}_{p,p'}+W^{(e\text{-}p)}_{p,p'}(1-f_{p'}(t))](x_{p'}-x_p+2L), \tag{15}$$

where the sum runs over x_p, $x_{p'}\in[0,2L]$. The terms proportional to $2L$ in the Eq. (15) take account of the motion of electrons out of and into the interval $[0,2L]$. They occur because f_p $[=f(x_p)]$ is periodic in the x direction with period $2L$ and $W^{\mathrm{Sch}}_{p,p'}$ and $W^{(e\text{-}p)}_{p,p'}$ have been defined for all p, p' corresponding to x_p, $x_{p'}\in[0,2L]$, but such that they also describe motion (scattering) across the two *boundaries* of the interval $[0,2L]$ whenever $|x_{p'}-x_p|>L$, see Appendix D.

In the *steady state* (which is defined by $\partial f_p/\partial t=0$ for all p) the Hall current density (15) has the simplified form

$$j_x=[e/(L_y)]\left(\sum_{\substack{p,p'\\ x_{p'}-x_p>L}}f_p(t)[W^{\mathrm{Sch}}_{p,p'}+W^{(e\text{-}p)}_{p,p'}(1-f_{p'}(t))]\right.$$

$$\left.+\sum_{\substack{p,p'\\ x_p-x_{p'}>L}}f_p(t)[W^{\mathrm{Sch}}_{p,p'}+W^{(e\text{-}p)}_{p,p'}(1-f_{p'}(t))]\right). \tag{16}$$

Here two remarks are important. The transition rates $W^{\mathrm{Sch}}_{p,p'}$ are expressed in terms of the Zener transition probabilities (8), see Appendix B, and thus *contain all orders with respect to* E_y. In particular, those of the $W^{\mathrm{Sch}}_{p,p'}$ which give a major contribution to ''hoppings'' from an x_p on one slope of $V(x)$ to an $x_{p'}$ on the opposite slope are highly nonlinear in E_y. This means that the current across the top of a hill or the bottom of a valley of $V(x)$ (i.e., across the regions of insulating states) is entirely due to such nonclassical velocity components. In other words, any nonzero Hall current in the steady state contains such nonclassical, nonlinear contributions. This is true, in particular, for the macroscopic Hall current in the quantized plateau regime. This current is linear in E_y. But on a microscopic level the individual particle velocities of the conducting states are composed of linear *and* nonlinear (time-dependent) components[6(a)–6(f)] (see also the remark in the second last paragraph of Sec. VI).

The other possible contribution to j_x due to ''hoppings'' between the localized states ψ_p arises from the transition rates $W^{(e\text{-}p)}_{p,p'}$. In Sec. VI we will see that these phonon induced contributions increase the plateau width of σ_{xy} at low temperatures.

V. CONDUCTIVITIES

The experimentally relevant current densities are obtained from the *steady-state solution* of Eq. (11). The conductivities are then given by $\sigma_{yy}=j_y$(steady state)$/E_y$ and $\sigma_{xy}=j_x$ (steady state)$/E_y$.

As a result of the form of $V(x)$, the k dependence of the energies of the two-dimensional electrons, $E[k_y(p)]=V(x_p)+\text{const}$, is analogous to the dispersion relation $\varepsilon(k)$ of one-dimensional Bloch electrons. Therefore, Eq. (12) resembles the Boltzmann equation of Bloch electrons interacting with acoustic phonons, which is a standard model for the *dissipative* electric conductivity of metals or semiconductors.[16] However, in those derivations the Schrödinger time evolution is supposed to be either unperturbed classical (or quasiclassical if a periodic substrate potential is present) [which in our model corresponds to $P_j=1$ for all energies E_j in the broadened Landau band], or the effect of the disorder potential is assumed to be sufficiently small (or, equivalently, $|\mathbf{E}|$ sufficiently high), such that the Schrödinger time evolution is not very far from the unperturbed classical or quasiclassical motion in an electric field [which in our case would mean $P_j\simeq 1$ for all j]. If then only terms linear in $\mathbf{E}$ are considered in the Boltzmann equation, and further, if the deviation f^1 of the steady state from the Fermi distribution f^0 is small ($f^1\ll 1$), an approximate solution for the steady state can be obtained (using, e.g., a relaxation time approximation).[16] This leads to a Drude-type relation for the dissipative conductivity (Ohm's law).

In our case we cannot make analogous approximations. First of all, for the considered value of E_y, the nonadiabatic transition probabilities P_j [which depend on E_y, see Eq. (8)] are equal or close to one only in the very center of the conducting range. Only here can the influence of the disorder potential term $V^1(x,y)$ on the Schrödinger time evolution be approximately neglected. This means that only around half-integer filling factors may one expect j_y to be approximately linear in E_y (provided f^1 is linear), see Eq. (C4).

Secondly, in our system f_p is quite different from f_p^0 when the Fermi energy is in the range of conducting states. The biggest deviation is of order 1 and occurs for half-integer filling of the band, see Fig. 1. The two underlying reasons are the following: First of all, in our system the velocities parallel to the macroscopic electric field are quite high for states near the band center, much higher than in typical experimental quantum Hall systems (as a consequence of the big value of $|V'(x_p)|$). This rapidly pushes these states (for which P_j is equal or close to 1) out of their energetic equilibrium position, towards higher (lower) energies on a positive (negative) slope [cf. Eqs. (11)–(13) and the equations of Appendix C]. Further, as a consequence of the condition $q_y\leqslant q$ (see Sec. III) elastic and quasielastic scattering with phonons from one slope to the opposite one are totally suppressed (the energy range of such forbidden slope changing processes starting from a given energy E_j increases towards the band center). These processes—which would interrupt most effectively the evolution away from $f^{(0)}$ caused by the field E_y and, therefore, would lead to a quick relaxation towards the equilibrium distribution f^0 if E_y was switched off, as in metals—are absent in our system.[18]

For these reasons the usual methods for finding an approximate analytical solution of the steady-state equation are not applicable in our case. Therefore Eq. (11) was solved numerically without approximations. This means that our results contain all orders with respect to the electric field E_y and are not restricted to a linear approximation (see also the remark in the second to the last paragraph of Sec. IV).

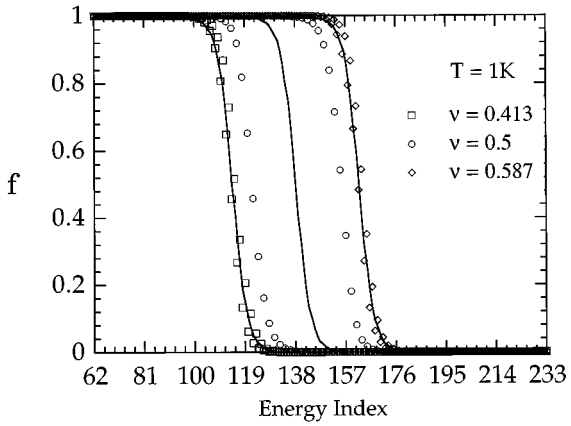

FIG. 1. The steady state distribution $f=f_p=f(E_p)$ at $T=1$ K for filling factors $\nu=0.413$ (squares), $\nu=0.5$ (circles), $\nu=0.587$ (diamonds), and the corresponding distributions in the absence of the electric field E_y (solid lines), which are Fermi distributions. See also text, Sec. VI. The band contains 276 states, symmetrically distributed with respect to the band center, which is situated beween energy indexes 138 and 139. (Note that in Figs 1–4, ν denotes the filling factor within the highest partially occupied Landau band.)

Note that if we did not couple the electronic system to a heat bath and if we considered the steady state of the Schrödinger time evolution in the presence of E_y in this case, we would obtain $\sigma_{yy}=0$ even for half-filling of the band, because in this case the Schrödinger time evolution is not interrupted by electron-phonon interactions and then leads to a steady state with equal occupation of all energies of the conducting states.[6(f)]

VI. NUMERICAL RESULTS AND DISCUSSION

For the numerical calculation of the present article we used the same labeling of the ψ_p as in Fig. 1 of Ref. 6(f), but we slightly shifted the origin of time by $+\tau/4$ keeping ε_p as the unperturbed energy E_p. This shift does not change any of the formulas derived in the present article, it only makes E_p (p odd) coincide with E_{p+1}. This means that now to each basis function ψ_p, p odd, with energy E_p, situated on a positive slope of $V(x)$ there exists another basis function ψ_{p+1} situated on the opposite slope, which has the *same* energy $E_{p+1}=E_p$ (p odd). This energetic symmetry has the advantage that the energies E_p of states on opposite slopes have exactly the same equilibrium (Fermi) distribution f_p^0 on each of the slopes separately.

If E_y is zero, all $W^{\text{Sch}}_{p,p'}(p\neq p')$ are zero as well (hence $j_x=0$), and the numerical solution of Eq. (11) becomes the corresponding Fermi distribution $f_p^0(T)$ as it should (see Fig. 1). Note that $f_p^0(T)$ is the same on each slope separately [$f_p^0(T)=f_{p'}^0(T)$ for $E_p=E_{p'}$ with x_p, $x_{p'}$ on opposite slopes of $V(x)$], whence $j_y=0$.

After switching on E_y, the Fermi distribution rapidly

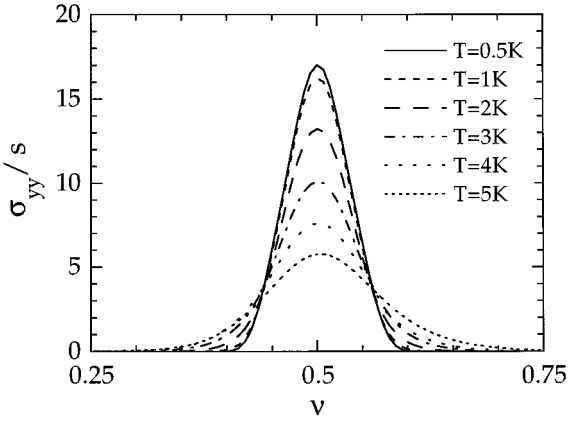

FIG. 2. Dissipative conductivity σ_{yy} at six different temperatures, as the function of the filling factor ν. Here $s=|v_y e/(2LL_y E_y)|=|V'c/2LL_y E_y B|$; compare Eqs. (14), (C2)–(C4).

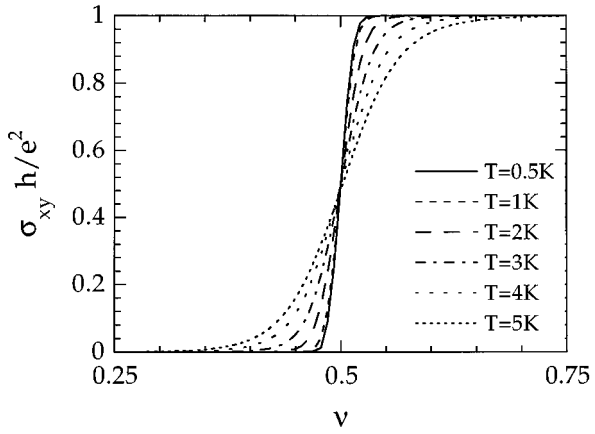

FIG. 3. Hall conductivity σ_{xy} at six different temperatures, as the function of the filling factor ν. Note that the plateaus are larger than those of σ_{yy} in Fig. 2.

goes over into the steady-state distribution $f(E_p)$. Figure 1 illustrates this for $T=1$ K. For each filling factor in the conducting range, $f(E_p)$ is composed of two branches, each of which is approximately a shifted Fermi distribution [shifted to higher (lower) energies for p odd, i.e., for states on a positive slope of $V(x)$ (for p even, i.e., for states on a negative slope)]. This shift is the highest for $\nu=1/2$ and tends to zero as ν approaches the mobility edges [to avoid confusion we note that in Figs. 1–4 ν denotes the filling factor only within the highest partially occupied band]. j_y is different from zero if the steady state distribution is different on two opposite slopes. This is the case, if ε_F is in the conducting range (where $P_p>0$). On the other hand, if ε_F lies sufficiently within the range of nonconducting states (where $P_p=0$), one obtains again the same Fermi distribution on both slopes, whence $j_y=0$.

The numerical results for the dissipative conductivity σ_{yy} are shown in Fig. 2. In order to appreciate these results, we first recapitulate some known features concerning the peak values observed in conventional MOSFET's and hetero junctions. Experiments performed over a wide range of temperatures down to 50 mK reveal a rather complex pattern.[19] For instance, below 10 K, the peak value $\sigma_{yy}^{\max}$ (i) first *increases* as the temperature is lowered, then (ii) around 1 K this tendency is reversed and the maximum value of σ_{yy} *decreases* as T goes down, until (iii) at the lowest temperatures the downwards slope levels out and the conductivity saturates.[20]

Our results can directly be compared to (i), since the phonon scattering mechanism employed in our paper is adequate at temperatures around 1–5 K. Although in our model system the density of states (a rectangular step function) and the disorder potential $V(x,y)$ are different from those in ordinary quantum Hall samples (and, in addition, we have neglected screening), we may take the results obtained as guidelines for an analysis. Our $\sigma_{yy}^{\max}$ goes down approximately linearly when T is increased, in qualitative accordance with (i). Further, the half-width of the σ_{yy} peak increases roughly as T^2 when T increases.

These two effects can be seen simply as a consequence of the broadening of $\partial f^0(E)/\partial E$ with increasing T [since the curves $f(E)$ of Fig. 1 turned out to be approximately ''split'' Fermi distributions], which leads to a larger contribution of the nonconducting states when ε_F is in the band center (i.e., to a decrease of the weight of the states with $P\approx 1$, which are in the band center). Hence $\sigma_{yy}^{\max}$ is reduced. On the other hand, if ε_F is near a mobility edge, more and more conducting states are included as T goes up, leading to the broadening of the σ_{yy} curve.

Figure 3 shows the calculated Hall conductivity σ_{xy} as a function of ν and T. One sees that on the left/right there are plateaus with the correct quantized values (0 and 1 in units of e^2/h). The transition region between the plateaus becomes narrower as T decreases, in qualitative agreement with the experimental situation. The main reason for this is the same as for the narrowing of the σ_{yy} curve.

In recent years considerable effort has been made to describe the temperature behavior of the conductivities between the plateaus by scaling laws.[2] Although most of the thus-far-investigated samples seem to follow these laws there are quite a few samples where a different behavior has been observed (see, e.g., Sec. II A of Refs. 2, 21, and 22). This sample dependence indicates that the temperature behavior may depend on the nature of the disorder potential, see, in particular, Refs. 21 and 22).

An important and perhaps more surprising result of our calculations is the following. We found that the plateau of σ_{xy} is larger than the plateau of σ_{yy}, especially at temperatures below 5 K (Figs. 2 and 3). This difference originates from the electron-phonon contribution to the Hall current (16), as can be seen from Fig. 4, where the Schrödinger contributions to $\sigma_{xy}(\nu)$ [containing the terms $W_{p,p'}^{\mathrm{Sch}}$ in Eq. (16)] and the electron-phonon contributions (containing the terms $W_{p,p'}^{(e\text{-}p)}$) are shown separately. Note that a difference in the width of the σ_{yy} and σ_{xy} plateaus is possible because, in contrast to the dissipative current (14), the Hall current (16) contains also terms that explicitly involve the electron-phonon transition rates $W_{p,p'}^{(e\text{-}p)}$.

This effect that the plateau of the Hall conductivity is somewhat larger than the plateau of the dissipative conductivity has also been observed in experiments (where usually the resistivities are measured). Indeed, since the early days of the IQHE many resistivity curves quite clearly show a larger

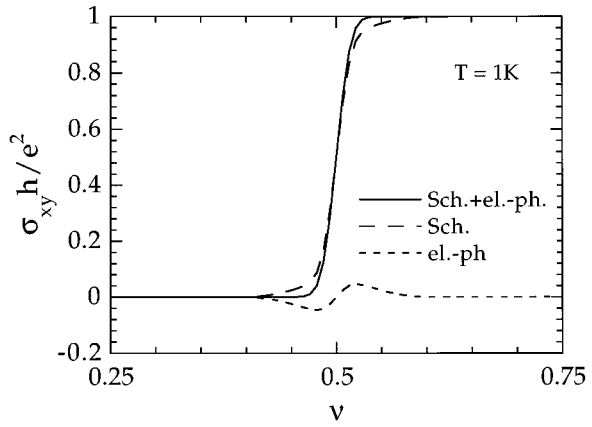

FIG. 4. Different contributions to the Hall current j_x, Eq. (16). Dashed line, terms containing the Schrödinger transition rates $W^{\mathrm{Sch}}_{p,p'}$; broken line, terms containing the electron-phonon transition rates $W^{(e\text{-}p)}_{p,p'}$; solid line total.

plateau for the Hall resistivity.[23] In conventional quantum Hall systems [where $(\sigma_{yy})^2 \ll (\sigma_{xy})^2$ for all filling factors] this is equivalent to a larger plateau of the Hall conductivity compared to the dissipative conductivity (see Fig. 1 of Ref. 24).

It seems that our microscopic calculation has revealed the physical origin behind this effect. We are not aware of any explanation given elsewhere in the literature.

Further, it appears that the Shubnikov–de Haas peak in our model does not tend to an exact δ function at $T=0$. This is in qualitative agreement with recent measurements on high- and low-mobility samples,[21] for which *a finite* width of the Shubnikov–de Haas peak was found at zero temperature, showing that more than one populated state is extended at $T=0$, which is also the case in our model system.

On the other hand it seems that our $\sigma_{xy}(\nu)$ curves do tend to a step function in the zero-temperature limit, as is usually expected. But in order to achieve this, the localization-delocalization properties of the Schrödinger functions, which are usually made responsible for this, seem not to be sufficient here but have to be complemented by phonon-assisted hopping between localized states.

When ε_F lies within the range of nonconducting states [condition (1) of Ref. 6(i)], i.e., when the steady state is again described by a Fermi distribution (see above and Fig. 1) and hence the dissipative current j_y is zero, the Hall current density j_x is entirely given by the Schrödinger part of Eq. (16), which in this case has the value $j_x = E_y(e^2/h)\times i$ (where i is the number of upper mobility edges of spin-split broadened Landau bands below ε_F).

Let us recall here that it has been shown analytically[6(i)] that, quite generally, the quantization $\sigma_{xy}=(e^2/h)\times i$ occurs whenever a disorder potential $V(x,y)$ combined with E_y gives rise to solutions of the time dependent Schrödinger equation, such that conditions (1) and (2) of Ref. 6(i) [conditions (a) and (b) of Ref. 6(j)] are fulfilled. These conditions are particularly transparent in our model system. Here the second condition is fulfilled due to the existence of an x_p across which the Schrödinger motion is entirely classical (i.e., for which the corresponding Zener probability P_p is equal to 1). For further details we refer to Refs. 6(i), 6(j), and, in particular, to Ref. 6(f), where the Schrödinger time evolution of the present model system and the resulting Hall current have been analyzed in detail. Reference 6(f) also contains a particularly detailed microscopic explanation of the key features of the IQHE in the framework of this model.

We emphasize that Eqs. (14) and (16) continuously describe σ_{yy} and σ_{xy} of our system over the whole range of filling factors from one quantized plateau through the dissipative range to the adjacent quantized plateau. It seems that such a consistent description of Hall conductance plateaus and dissipative region by a single theoretical prescription, based on the essentially exact time-dependent microscopic processes, has not been achieved elsewhere.

VII. CONCLUSIONS

We have investigated a system of electrons in a model disorder potential $V(x,y)$ (''toy model''), which interacts with the phonons of a heat bath. In this model system the basic processes involved in the transport properties of a quantum Hall system are illustrated in a transparent way. We believe that these processes qualitatively also represent those in the usual experimental systems (MOSFET's and heterojunctions), where the disorder potential is more complex.

We have provided the basic Eqs. (11), (14), and (16), which enable us to explicitly calculate the dissipative and Hall conductivities, starting from the Schrödinger equation and the electron-phonon interaction. These equations contain all the physical parameters of the system (filling factor, temperature, macroscopic electric field E_y, disorder potential, etc.). By solving the corresponding quantum Boltzmann equation (11) we obtained the conductivity plateaus with the correct quantized values and the conductivities between the plateaux consistently, i.e., with a single theoretical method and without introducing unproved assumptions. The physical parameters of the system that enter the expressions of the current densities are contained in the transition rates between the basis states $W^{(e\text{-}p)}_{p,p'}$ and $W^{\mathrm{Sch}}_{p,p'}$. The Schrödinger time evolution is described by the rates $W^{\mathrm{Sch}}_{p,p'}$, which depend not only on the disorder potential $V(x,y)$ but also on the macroscopic electric field E_y. All orders of the electric-field dependence are contained in our calculations (i.e., no linear approximation is made). The temperature dependence of the conductivities results from the temperature dependence of the transition rates $W^{(e\text{-}p)}_{p,p'}$, which describe the electronic motion induced by the electron-phonon interaction.

We believe that our calculation is of considerable didactical value for understanding what really goes on microscopically. In particular, our model illustrates the interplay between the full Schrödinger time evolution, which the electric field induces to the electron states in the broadened Landau band, and the time evolution resulting from the interaction with the phonons of a heat bath. This leads to an improved understanding of the region near the edges of the conductivity plateaus. Here crucial physics for the IQHE occurs, which determines the widths of the plateaus. Our analysis leads to an explanation of the difference in the plateau width of the Hall conductivity and of the dissipative conductivity. It seems that this widely observed phenomenon has not been explained before.

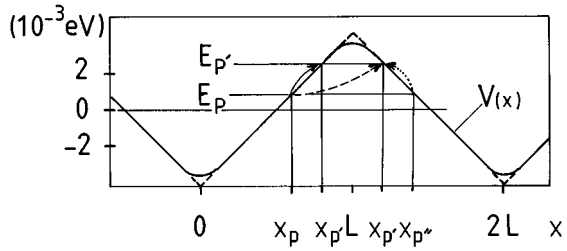

FIG. 5. Smooth disorder potential $V(x)$ with spatial period $2L = 1753$ Å. Solid arrow, slope conserving scattering process; dashed arrow, slope changing scattering process involving the same energy transfer; dotted arrow, its associated effective slope conserving process (see Appendix A).

In the framework of our model system, we have shown how a microscopic theory of the IQHE can be obtained, where all physical parameters are included consistently. Such a theory has been missing so far, even for a model system.

Our method of calculation may serve as a guideline towards the ultimate goal of a complete predictive theory of the IQHE. Future work along this line will have to extend our method to disorder potentials that are closer to those present in usual quantum Hall samples. Further, electron-electron interaction (screening) will have to be included, which, once done, will immediately lend itself to a more elaborate treatment of both DA and PA interactions, too. The latter, in turn, would allow one to attain lower T [cases (ii) and (iii) of Sec. VI], where the finite width of the Fermi distribution no longer masks the effects that manifest themselves in the scaling behavior of the conductivities.[2]

APPENDIX A

Let us determine the possible phonon wave vectors $\mathbf{q}$ that can scatter an electron from the initial state $k_y(p) = k_y(x_p) := k_y$ to the final state $k_y(p') = k_y(x_{p'}) := k_y'$. A ''unit cell'' of length $2L$ of the smooth potential $V(x)$ is depicted in Fig. 5. The repetition of this segment gives the potential in the whole sample. [For the numerical calculations we will use a constant slope $|V'(x)|$ from top to bottom of the hills (valleys) of $V(x)$, as shown by the broken line in Fig. 5.] This simplifies the calculations and the formulas, but does not affect the results of this paper since in our model the states outside the central, conducting region remain nonconducting, independent of the particular form of $V(x)$ near the top of a hill or bottom of a well. Further, we are mainly interested in a narrow region around the band center (the conducting states), but since T is very low, the conducting states cannot be excited to the very band edge.

As an example, we will consider the situation where the electron is initially on the upper left half-slope at position x_p, with the corresponding momentum $k_y = 2\pi p/Ly$ and emits (absorbs) a phonon of wave vector $\mathbf{q}$ and energy $\hbar\omega_{q'} = \hbar\overline{c_L}q$ ($\overline{c_L}$ is the average sound velocity) such that (a) the final position $x_{p'}$ is still on the *same* slope. The total energy and the y component of the momentum are conserved. Since $k_y' - k_y = 2\pi(p'-p)/L_y = (x_{p'} - x_p)/\lambda_B^2$, using Eqs. (6), (7), and (C3) we obtain

$$E(k_y') - E(k_y) = \hbar v_y(k_y)[k_y' - k_y], \tag{A1}$$

where $v_y(k_y)$ is $-v_y(v_y)$ on the left (right) slope. Together with Eq. (A1), the two conservation laws yield the following simple relation between q_y and q:

$$q_y = \pm\frac{\overline{c_L}}{v_y}\,q. \tag{A2}$$

This means that the phase space available to the phonons is restricted to the lateral surface of a cone with opening angle 2θ, where $\cos\theta = \overline{c_L}/v_y$. It will be convenient to express all the q-dependent quantities in terms of q_y. For a given q_y, all the $\mathbf{q}$-s the end points of which lie along the perimeter of a circle of radius $r = q_y(v_y^2/\overline{c_L^2} - 1)^{1/2}$ in the q_x-q_z plane around the q_y axis are allowed, and their different contributions to the transition probability must be summed up. We write the $\mathbf{q}$-space volume element in the form $d\mathbf{q} = dq_y r\,dr\,d\phi$. For simplicity we take now the dimensions of the bulk crystal to be $L_x = L_y = L_z$. Then $dq_y \approx \Delta q_y = (2\pi/L_x)$ and we may write $dr \simeq \frac{1}{2}(\Delta q_x + \Delta q_z) = (2\pi/L_x)$. The δ function in the Fermi golden rule result will be replaced by the inverse density of states, $\Delta\varepsilon^{-1}$, a constant in our system ($\Delta\varepsilon$ is the energy difference between two states with adjacent positions on a slope). The inplane and z component of the phonon wave vector $\mathbf{q}$ can be expressed as

$$q_\perp^2 = q_y^2\left[\frac{v_y^2}{\overline{c_L^2}} - \left(\frac{v_y^2}{\overline{c_L^2}} - 1\right)\sin^2\phi\right], \quad q_z^2 = q_y^2\left(\frac{v_y^2}{\overline{c_L^2}} - 1\right)\sin^2\phi. \tag{A3}$$

The ϕ-dependent terms can then be lumped together in one integral $I(q_y)$ (the bar denotes the summation over ϕ), and the rest of the (partially summed) transition probability can be incorporated into a prefactor that will be called $F(q_y)$ (see below).

(b) A somewhat different scenario arises when the final state is on the opposite (upper right) half-slope. Let us first look at the site opposite to the previous $x_{p'}$, marked by the dashed arrow in Fig. 5. For this new $x_{p'}$, the energy change ($\propto q$) is the same as in (a), but the momentum change ($\propto q_y$) is clearly much bigger. For such slope changing processes, it proves to be advantageous to define an effective scattering process (dotted arrow in Fig. 5) with the same q, but an effective $\tilde{q}_y$ on the slope of the final state

$$\alpha_{p,p'} = \frac{|x_{p'} - x_p|}{|x_{p''} - x_{p'}|} = \frac{q_y}{\tilde{q}_y}. \tag{A4}$$

Note that $\alpha_{p,p'} = 1$ for x_p, $x_{p'}$ on the same slope. With this, Eq. (A2) is replaced by

$$q_y = \pm\,\alpha_{p,p'}\,\frac{\overline{c_L}}{v_y}\,q. \tag{A5}$$

As a consequence, $\overline{c_L}$ in Eq. (A3) must be replaced by $\alpha_{p,p'}\overline{c_L}$. Finally, replacing q_y by $\tilde{q}_y$ using Eq. (A4), the ϕ integral takes the form

$$\overline{I}(\tilde{q}_y,\alpha_{p,p'},\lambda_z) = 4\exp\left(-\frac{1}{2}\lambda_B^2\tilde{q}^{\,2}_y\tilde{v}^{\,2}\right) \times\int_0^{\pi/2}\frac{\exp\left(\frac{1}{2}\lambda_B^2\tilde{q}^{\,2}_y(\tilde{v}^{\,2}-\alpha^2_{p,p'})\sin^2\phi\right)}{(1+\lambda_z^2\tilde{q}^{\,2}_y(\tilde{v}^{\,2}-\alpha^2_{p,p'})\sin^2\phi)^3}d\phi, \tag{A6}$$

where $\tilde{v}$ denotes $v_y/\overline{c_L}$ (=4.15 at $B=6T$ in our model).

Further, the prefactor becomes

$$F(\tilde{q}_y,\alpha_{p,p'})=\frac{\Xi_d^2\sqrt{\tilde{v}^{\,2}-\alpha^2_{p,p'}}}{2\rho\overline{c_L^2}L_x h}\tilde{q}^{\,2}_y, \tag{A7}$$

where ρ (5.31×10^3 kgm^{-3}) is the volume density of the crystal and Ξ_d (7 eV) is the bulk deformation potential coupling constant.[25] In the denominator we used that $\Delta\varepsilon L_y = V'(x)|x_p-x_{p-1}|L_y=hv_y$, with h being Planck's constant. For simplicity only a single longitudinal acoustic mode and an average sound velocity of $\overline{c_L}$ (4.03×10^3 ms^{-1}) has been considered.

The calculation is similar if x_p is on the other three half-slopes, and the form of Eqs. (A6) and (A7) remains the same. We remark that the probability of scattering along a distance $2L$ or beyond is negligible and the corresponding transition probabilities are set equal to zero. Further, $W^{(e\text{-}p)}_{p,p'}$ is zero if $\alpha_{p,p'}>\tilde{v}$. This latter inequality is equivalent to $q_y>q$, which is physically not possible.

APPENDIX B

The $W^{\rm Sch}_{p,p'}$ are the Schrödinger transition probabilities per unit time to go from a basis state ψ_p to a state $\psi_{p'}$ during the time interval τ. Such a time evolution is described by the multiplication of two 2×2 matrices corresponding to two consecutive splittings. Therefore, the $W^{\rm Sch}_{p,p'}$ can be expressed in terms of the Zener probabilities (8) associated with these splittings. For instance, using the same labeling of the basis functions ψ_p as in Fig. 1 of Ref. 6(f) [where p odd (even) belong to x_p on positive (negative) slopes of $V(x)$], it is straightforward to obtain the following values for p odd,

$$W^{\rm Sch}_{p,p+2}=P_pP_{p+1}/\tau, \tag{B1a}$$

$$W^{\rm Sch}_{p,p+1}=P_p(1-P_{p+1})/\tau, \tag{B1b}$$

$$W^{\rm Sch}_{p,p-1}=(1-P_p)P_{p-1}/\tau \tag{B1c}$$

and for p even,

$$W^{\rm Sch}_{p,p-2}=P_{p-1}P_{p-2}/\tau, \tag{B2a}$$

$$W^{\rm Sch}_{p,p-1}=P_{p-1}(1-P_{p-2})/\tau, \tag{B2b}$$

$$W^{\rm Sch}_{p,p+1}=(1-P_{p-1})P_p/\tau. \tag{B2c}$$

The diagonal elements $W^{\rm Sch}_{p,p}$ are irrelevant, since they do not appear in (or fall out of) any of the relevant Eqs. (11), (14)–(16). Note that in our explicit calculation $P_p=0$ for $|p|\geqslant28$. Hence $W^{\rm Sch}_{p,p'}(p\neq p')=0$ for $p\leqslant-28$ or $p>28$. This means that the lower and upper *mobility edges* are situated at the energies E_{-28} and E_{28}, respectively. The transition rates $W^{\rm Sch}_{p,p'}$ (which are determined by the nonadiabatic transition probabilities P_p) are an important element in the determination of the velocities (14) parallel to the macroscopic electric field E_y, and of the Schrödinger contribution to the velocities perpendicular to E_y [see Eqs. (11) and (16)].

We recall that through the P_p, which are given by Eq. (8), the transition rates $W^{\rm Sch}_{p,p'}$ explicitly depend on the physical parameters of the system, in particular, on the disorder potential $V(x,y)$ and on the absolute value of the macroscopic electric field E_y. This means that the mobility edges are determined by the form of $V(x,y)$ *and* by the absolute value of E_y.

APPENDIX C

Expression (14) for the current density in the y direction can be expressed in terms of the individual velocities in the y direction of the basis states ψ_p. We take again the same numbering of the basis states ψ_p as in Ref. 6(f). Let us consider p odd. In this case $W^{\rm Sch}_{p,p'}$ differs from zero only for $p'=p+2$, $p-1$, and $p+1$; see Appendix B. For instance, for $p'=p+2$ we have $W^{\rm Sch}_{p,p+2}=P_pP_{p+1}/\tau$. Further, $E_{p+2}-E_p=V'(x_p)cE_y\tau/B$; hence in the sum (14) we have

$$W^{\rm Sch}_{p,p+2}(E_{p+2}-E_p)/(qE_y)=[V'(x_p)c/(eB)]P_pP_{p+1}, \tag{C1}$$

where

$$[V'(x_p)c/(eB)]=v_y^p \tag{C2}$$

is just the velocity in the y direction of an unperturbed Landau function ψ_p at the position x_p (i.e., of a basis function ψ_p in the absence of E_y). In our model system the velocities v_y^p have all the same absolute value,

$$v_y=|[V'(x_p)c/(eB)]|, \tag{C3}$$

and their sign is negative if x_p is on a slope with positive V' and vice versa (note that the electronic charge e is negative).

By analogous considerations for the remaining p,p', expression (14) can be written as

$$j_y=[e/(2LL_y)]\left\{\sum_{p\ \rm odd}v_y^pf_p[P_pP_{p+1}+P_pP_{p-1}-P_{p-1}] + \sum_{p\ \rm even}v_y^pf_p[P_{p-1}P_{p-2}+P_{p-1}P_p-P_p]\right\}. \tag{C4}$$

Equation (C4) is an explicit sum over all conducting states in our model system. These states are characterized by $P_p\neq0$. Since in our explicit example $P_p=0$ for $|p|\geqslant28°$, the sum (C4) is therefore restricted to $-27\leqslant p\leqslant27$ (p odd), $-26\leqslant p\leqslant28$ (p even). We recall that the mobility edge at $|p|=28$ is determined by the form of $V(x,y)$ *and* by the absolute value of E_y. The mobility edges can be shifted by changing at least one of these physical parameters. For instance, increasing E_y in Eq. (8) shifts the mobility edges towards the band tails. This is a general phenomenon in

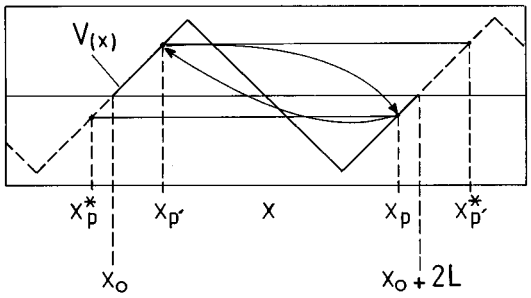

FIG. 6. Schematic illustration to Appendix D. Shown are two localization centers $x_p, x_{p'}$, both contained in the unit cell of $V(x)$ of length $2L$ (full line), and for which $|x_{p'}-x_p| \geq L$. Hence the two corresponding scattering processes (indicated by arrows) are negligible in our system. The corresponding (vanishing) matrix elements $W_{pp'}$ and $W_{p'p}$ are then replaced by the transition rates corresponding to the scattering between $x_p, x_{p'}^*$, and $x_{p'}, x_p^*$, respectively.

quantum Hall systems and lies at the origin of the high current breakdown of the IQHE [Refs. 6(h) and 6(i)].

APPENDIX D

Figure 6 schematically shows the energies E_p and the associated localization centers x_p of the orbitals ψ_p. The system is infinitely long in the x direction and periodic with a period $2L$. The $W_{p,p'}$ are the transition rates among the basis functions ψ_p, each of which is localized at its site x_p. The total occupation probabilities f_p of the sites x_p are periodic as well. They are determined from the Boltzmann equation (12) through the transition rates $W_{p,p'}$ ($W_{p,p'}^{\mathrm{Sch}}$, or $W_{p,p'}^{(e\text{-}p)}$) which decrease exponentially with the distance $|x_p - x_{p'}|$. In our system the $W_{p,p'}$ can be neglected for distances $|x_p - x_{p'}| \geq L$. Then the Boltzman equation can be written in a periodic form by restricting it to the N ($=276$) basis states ψ_p with positions x_p in the unit cell $[x_0, x_0+2L]$. The $W_{p,p'}$ are then the elements of an $N \times N$ matrix, which formally describe the transitions among these N basis functions. They describe the real transitions among two positions $x_p, x_{p'}$ only if $|x_p - x_{p'}| < L$, whereas for positions $x_p, x_{p'}$ with $2L > |x_p - x_{p'}| \geq L$, the real matrix elements $W_{p,p'}$ (which are zero, see above) are replaced by the matrix elements for the corresponding processes involving the same energy change *across* the point x_0 (or equivalently, *across* x_0+2L) see Fig. 6. This means that in our $N \times N$ matrix, the element $W_{p,p'} = W(x_p, x_{p'})$ is replaced by $W(x_p, x_p^*)$, and $W_{p',p} = W(x_{p'}, x_p)$ is replaced by $W(x_{p'}, x_p^*)$, where the points x_p, $x_{p'}$, x_p^* and $x_{p'}^*$ are shown in Fig. 6. The resulting $N \times N$ matrix describes the evolution in the infinitely extended system.

[1] K. von Klitzing, G. Dorda, and M. Pepper, Phys. Rev. Lett. **45**, 494 (1980).

[2] B. Huckestein, Rev. Mod. Phys. **67**, 357 (1995) (reviews the scaling theory of the IQHE including experimental results).

[3] M. Janssen, O. Viehweger, U. Fastenrath, and J. Hajdu, *Introduction to the Theory of the Integer Quantum Hall Effect* (VCH, Weinheim, 1994) (emphasizes linear response theory).

[4] B. Kramer and A. MacKinnon, Rep. Prog. Phys. **56**, 1469 (1993) (review about disordered electronic systems and localization).

[5] H. Scherer, L. Schweitzer, F. J. Ahlers, L. Bliek, R. Lösch, and W. Schlapp, Semicond. Sci. Technol. **10**, 959 (1995).

[6] (a) J. Riess, Z. Phys. B **77**, 69 (1989); (b) Phys. Rev. B **41**, 5251 (1990); (c) J. Phys. (France) **51**, 815 (1990); (d) J. Riess and C. Duport, J. Phys. I **1**, 515 (1991); (e) J. Riess, in *High Magnetic Fields in Semiconductor Physics III*, edited by G. Landwehr, Springer Series in Solid State Science Vol. 101 (Springer-Verlag, Berlin, 1992), p. 94; (f) D. Bicout, P.-A. Hervieux, and J. Riess, Phys. Rev. B **46**, 9577 (1992); (g) J. Riess and P. Magyar, Physica B **182**, 149 (1992); (h) J. Riess, *ibid.* **190**, 366 (1993); (i) **204**, 124 (1995); (j) in *High Magnetic Fields in the Physics of Semiconductors*, edited by D. Heiman (World Scientific, Singapore, 1995), p. 165; (k) Z. Naturforsch. Teil A **50**, 1090 (1995).

[7] The adiabatic theorem is discussed in A. Messiah, *Quantum Mechanics* (Wiley, New York, 1966), Vol. II, Chap. XVII.

[8] There may be an exception: If the particle number N is odd, the adiabatic state in the very center of the spectrum may have a nonzero averaged Hall velocity (v_x). In our case, however, N is even and the time averaged velocities in the y and x directions are zero for all adiabatic states of the broadened Landau band.

[9] H. Aoki and T. Ando, Solid State Commun. **38**, 1079 (1981).

[10] F. Dietzel, W. Dietsche, and K. Ploog, Phys. Rev. B **48**, 4713 (1993); Y. Okuyama and N. Tokuda, *ibid.* **40**, 9744 (1989).

[11] S. Tamura and H. Kitagawa, Phys. Rev. B **40**, 8485 (1989); T. Brandes, Phys. Rev. B **52**, 8391 (1995).

[12] T. Ando, A. B. Fowler, and F. Stern, Rev. Mod. Phys. **54**, 437 (1982) and references therein.

[13] See, e.g., B. K. Ridley, *Quantum Processes in Semiconductors* (Clarendon, Oxford, 1982), Chap. 3.

[14] H. L. Zhao and S. Feng, Phys. Rev. Lett. **70**, 4134 (1993). Note the interchange of the x-y axes, and the misprint in the argument of the exponential.

[15] V. F. Gantmakher and Y. B. Levinson, in *Carrier Scattering in Metals and Semiconductors*, edited by A. A. Grinberg and S. Luryi (North-Holland, Amsterdam, 1987), p. 353.

[16] See, e.g., H. Haken, in *Quantum Field Theory of Solids* (North-Holland, Amsterdam, 1976), Sec. 31; N. W. Ashcroft and N. D. Mermin, *Solid State* Physics (Holt, Rinehart and Winston, New York, 1976), Chap. 13.

[17] J. Riess, Phys. Rev. B **38**, 3133 (1988).

[18] Sometimes when symmetry considerations forbid, or conservation theorems suppress, all first-order transitions, second-order processes involving transitions via virtual states may open up new scattering channels. It was checked that this is not the case here.

[19] M. A. Paalanen, D. C. Tsui, and A. C. Gossard, Phys. Rev. B **25**, 5566 (1982); and Ref. 2.

[20] In this context it is to be noted that a stronger, and sometimes qualitatively different, T dependence of the peaks corresponding to the lower Landau levels was often observed; see, e.g., S. Kawaji and J. Wakabayashi, J. Phys. Soc. Jpn. **56**, 21 (1987).

[21] P. J. Gee, R. D. Leadly, S. O. Hill, J. Singleton, R. J. Nicholas, J. J. Harris, and C. T. Foxon, *High Magnetic Fields in the Physics of Semiconductors*, edited by D. Heiman (World Scientific, Singapore, 1995), p. 252.

[22] F. W. Van Keuls, H. W. Jiang, and A. J. Dahm, Czech. J. Phys. **46**, Suppl. S5, 2467 (1996).

[23] See, e.g., K. von Klitzing, B. Tausendfreud, H. Obloh, and T. Herzog, in *Proceedings of the International Conference on Application of High Magnetic Fields in Semiconductor Physics, Grenoble, France, 1982*, edited by G. Landwehr, Lecture Notes in Physics Vol. 177 (Springer, Berlin, 1983), p. 1, Fig. 6.

[24] D. Shahar, D. C. Tsui, M. Shayegan, E. Shimshoni, and S. L. Sondhi, Phys. Rev. Lett. **79**, 479 (1997).

[25] The use of the bulk constant and the neglection of screening (Ref. 9 does not screen) has recently been questioned by I. Gorczyca and J. Krupski, Phys. Rev. B **52**, 11 248 (1995). This has no direct bearing on our results, and in any case is beyond the scope of the present approach.